Dynamical Ordering of Driven Stripe Phases in Quenched Disorder

C. Reichhardt, C. J. Olson Reichhardt, I. Martin, and A. R. Bishop

CNLS, Theoretical Division and Applied Physics Division, Los Alamos National Laboratory, Los Alamos, New Mexico 87545

(Received 30 August 2002; published 16 January 2003)

We examine the dynamics and stripe formation in a system with competing short and long-range interactions in the presence of both an applied dc drive and quenched disorder. Without disorder, the system forms stripes organized in a labyrinth state. We find that, when the disorder strength exceeds a critical value, an applied dc drive can induce a dynamical stripe ordering transition to a state that is more ordered than the originating undriven, unpinned pattern. We show that signatures in the structure factor and transport properties correspond to this dynamical reordering transition, and we present the dynamic phase diagram as a function of strengths of disorder and dc drive.

DOI: 10.1103/PhysRevLett.90.026401 PACS numbers: 71.45.Lr, 64.60.Cn, 73.20.Qt, 89.75.Kd

Recently, there has been considerable interest in the dynamics of driven elastic media in the presence of quenched disorder and an applied drive. Physical systems that fall into this category include vortex lattices in disordered superconductors [1–8], sliding charge-density waves [9], driven electron crystals in the presence of random impurities [10], sliding friction [11], and domain wall motion [12]. One of the most studied systems in this class is a vortex lattice driven by an applied current through disordered superconductors. Higgins and Bhattacharya [1] used transport measurements to map out a dynamical phase diagram for driven vortex matter based on transport signatures, and proposed the existence of three dynamical phases: a low drive pinned phase where the vortices do not move, a plastic phase where inhomogeneous flow and tearing of the highly disordered vortex lattice occurs, and an elastic flow regime where the lattice slides as a whole [1]. Koshelev and Vinokur [2] investigated the driven vortex lattice system theoretically and numerically, observed three phases as a function of increasing applied drive, and found that the disordered lattice in the plastic flow regime can undergo a striking *dynamical freezing* transition in which the vortex lattice *reorders* at high drives.

Further theoretical work has shown that the recrystallized state is not fully ordered but is still strongly affected by transverse modes from the pinning. Thus, the reordered state may form a moving smectic lattice with anisotropic ordering, where the vortices move in one-dimensional (1D) partially coupled channels aligned with the drive [3–5]. This reordering transition to an aligned moving smectic state has been experimentally confirmed by transport [6] and direct imaging [7] experiments. In addition, numerical work has confirmed the presence of a field-driven plastic to ordered or elastic transition [8]. Dynamical reordering has also been studied in sliding charge-density waves [9] and driven Wigner crystals [10].

A natural question is whether these dynamical phases and reordering transitions can occur in other systems which do not form triangular lattices in the absence of quenched disorder. For example, many systems form "stripe" or "labyrinth" states [13], including diblock copolymers, magnetic domain walls [14], flux in type-I superconductors, water-oil mixtures [15], and charge ordered or electron-liquid crystal states in 2D electron gases [16,17] or superconductors [18]. These stripelike phases may be disordered or destroyed by quenched disorder. With an applied drive, however, it may be possible to return to a partially ordered state. One intriguing possibility is that the reordered state may be fully aligned with the drive, meaning that the moving ordered state would be *more ordered* than the stationary state observed without quenched disorder. This effect could be useful for straightening a labyrinth forming system when 1D arrays of aligned stripes are the desired pattern.

Here, we model a labyrinth or stripe forming system in 2D by conducting molecular dynamics simulations of interacting particles that have a long-range Coulomb repulsion and a short range exponential attraction. Such a system has previously been shown to produce stripe, bubble, and crystalline phases depending on the particle density and the relative strength of the attractive interaction [18,19]. We use overdamped dynamics which should be appropriate for systems such as colloids and magnetic domains. We do not take into account possible hydrodynamic effects. The equation of motion for a particle i is $\mathbf{f} = \mathbf{f}_{ij} + \mathbf{f}_p + \mathbf{f}_d = \eta \mathbf{v}_i$. Here, $\mathbf{v}_i$ is the particle velocity, η is the damping term which we set to unity, and the force from the other particles is $\mathbf{f}_{ij} = -\sum_j \nabla U(r)$, where

$$U(r) = \frac{1}{r} - Be^{-\kappa r}.$$

For small r, the repulsive Coulomb term dominates. To avoid a divergence of the Coulomb term, we cut off the force at very short distances ($r \leq 0.1$) which does not affect any of the results presented here. We also use a numerically efficient summation method for the long-range Coulomb interaction [20]. The force from the

quenched disorder $\mathbf{f}_p$ comes from N_p randomly placed attractive parabolic pins of maximum strength f_p and radius $r_p = 0.3$. The driving term $\mathbf{f}_d$ is applied in small increments of 0.02 up to $F_d = 6.0$. We measure the resulting particle velocities $V_x = \sum \mathbf{v}_i \cdot \hat{\mathbf{x}}$ by averaging the velocities at each f_d increment value for 1000 time steps. We fix $B = 1.25$ and choose a particle density $n_i = 0.128$ at which the equilibrium state in the absence of pinning is a labyrinth phase, rather than oriented stripes, which is consistent with the idea that stripe forming systems contain self-generated randomness [16]. The initial state is prepared by annealing from a high temperature molten state to $T = 0$. We conduct a series of simulations for varied f_p and N_p, with the number of particles $N_i = 1280$ and the system size $L = 100$. We have also run simulations for fixed n_i at various L and N_i, and find that only the transient responses are affected.

We first consider the case for fewer pinning sites than particles, $N_p = 400$. After annealing, we observe a distorted labyrinth pattern. Upon applying a drive, we find that there is no pinning threshold within our resolution and that the motion initially occurs by interstitial flow of unpinned particles around the particles that are trapped at the pinning sites. The overall velocity V_x is still less than the free flow velocity since a portion of the particles remain pinned. As the drive increases, the system becomes increasingly disordered and signatures of the labyrinth ordering are further lost. The flow in this regime consists of river structures where the particles flow in individual channels, similar to those observed in vortex systems [8]. Increasing the drive, we find that the system can reorder into *two distinct moving states*: (i) For *weak disorder*, the system reorders into a labyrinth state similar to the pattern that forms if the system is annealed and without quenched disorder. (ii) For sufficiently *strong disorder*, the particles reorder into a stripe state that is *aligned* in the direction of the drive. In Fig. 1, we show the real space images and the corresponding structure factor $S(k)$ for these phases.

In Fig. 1(a), the moving labyrinth phase shows stripe-like features which have no long-range orientation. The structure factor has an inner ring of width corresponding to the spacing between the stripes. The ring shape reflects the fact that the stripes do not have a particular orientation. The outer ring in $S(k)$ corresponds to the length scale of the lattice of individual particles that forms within each stripe. This tendency to form a lattice is reflected by some remnant of sixfold order in the outer ring. We find the same $S(k)$ characteristics for both the moving and stationary labyrinth states. In Fig. 1(c), we show the real space image of the particles in the interstitial flow region. Here the system is much more strongly disordered than the labyrinth regime. There are areas where the particles form moving channels, one particle wide, aligned in the direction of drive. The structure factor [Fig. 1(d)] is much more diffuse, reflecting the stronger disordering. There are, however, now two peaks for small k, which is due to the smectic ordering of the chain structures. In Fig. 1(e), we show the high drive state for strong disorder, where an ordered stripe state forms aligned in the direction of the drive. The corresponding structure factor in Fig. 1(f) shows two peaks for small k corresponding to the smectic ordering of the stripes, in contrast to the ring structure observed in the labyrinth phase. Additionally, the outer ring shows considerable sixfold modulations, due to the individual particles within the stripe forming a crystal structure.

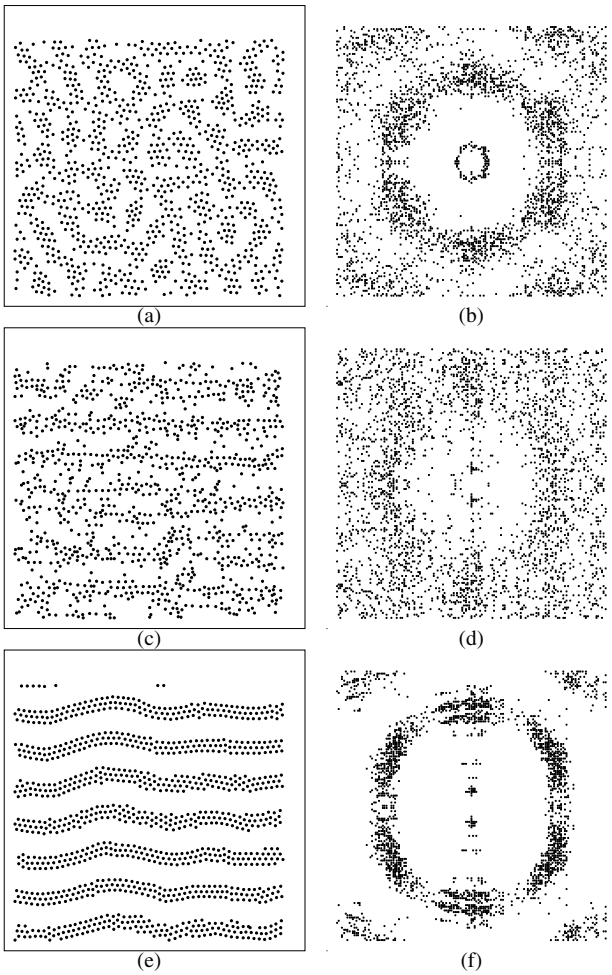

FIG. 1. (a),(c),(e) Real space images of the particle locations; (b),(d),(f) corresponding structure factor $S(k)$ for the following: (a),(b) the moving labyrinth phase for $f_p = 0.5$; (c),(d) the interstitial flow regime for $f_p = 6.5$; (e),(f) the moving stripe regime for $f_p = 6.5$. In each case the number of particles $N_i = 1280$ and pinning sites $N_p = 400$.

The oriented stripe state for strong disorder is consistent with studies for vortex matter in 2D where, for strong disorder, the vortices form a smectic state with ordering occurring in only the transverse direction. For weaker disorder, the vortex lattice anisotropy is reduced and the moving vortex lattice resembles the unpinned equilibrium state. The stripe ordering can also be viewed as a shear induced ordering. Shear forces are known to cause alignments into smectic phases [21]. In our case there is

no global shear, but there can be local shear if a portion of the particles remain pinned while other particles slide past. For weak disorder, the local shear forces are too weak to cause a realignment of the stripes.

We next show that the onset of the different phases strongly affects the transport properties. Additionally, we show that a convenient order parameter is the fraction P_6 of sixfold coordinated particles. For a perfect triangular lattice $P_6 = 1.0$. We find that the stripe and labyrinth phases have distinct P_6 values near 0.6 ± 0.015 and 0.5 ± 0.3, respectively, while the disordered phase has $P_6 < 0.5$. In Fig. 2(a), we plot the velocity V_x vs F_d for a sample with strong disorder, $f_p = 6.5$, along with the corresponding dV_x/dF_d curve (solid line). In Fig. 2(b), we show the corresponding P_6 vs F_d. There is a prominent peak in dV_x/dF_d near $F_d = 1.4$ and a second prominent peak near $F_d = 2.5$, with the latter peak corresponding to a rise in P_6 near $F_d = 2.5$. For $F_d < 1.5$, the system is disordered and only interstitial particles move through individual channels. For $1.5 < F_d < 2.5$, the system is still highly disordered, as seen from the low value of $P_6 \approx 0.35$. The flow now occurs throughout the sample, with individual particles intermittently escaping briefly from pins, and then being repinned. The first peak in dV_x/dF_d corresponds to the increase in V_x caused by the previously pinned particles depinning and taking part in the motion. The additional small peaks in dV_x/dF_d correspond to specific portions of the pinned particles breaking free and becoming mobile in 1D chains. Similar small peaks in dV_x/dF curves observed for driven vortices are believed to correspond to the depinning of large clumps of vortices [1,6]. The peak near $F_d = 2.5$ corresponds to the initial formation of the labyrinthlike stripe state, which is also seen as a sharp rise in P_6 to around 0.53. The stripe phase is fully formed for $F_d = 3.0$ where P_6 plateaus at $P_6 = 0.6$. The peak in dV_x/dF appears because the effectiveness of the pinning decreases as the stripes align. The dV_x/dF_d curve saturates to a constant value, reflecting free flow Ohmic behavior. We find the same features for other simulations for $2.5 < f_p$. For weaker pinning where a moving labyrinth forms, the dV_x/dF_d curves show only one prominent peak [shown in the inset of Fig. 2(b)] corresponding to the initial formation of the moving labyrinth. For driven vortex lattices, only one prominent peak is observed in the dV_x/dF curves when the vortex lattice reorders and makes a transition from the plastic flow phase to the Ohmic regime. We also find considerable hysteresis in the $V_x - F_d$ curves in the oriented stripe phase, while there is no hysteresis for the system with weak disorder.

In Fig. 3, we show the dynamic phase diagram for F_d vs f_p for $N_p = 400$. We delineate four phases: the interstitial phase, determined from the dV_x/dF_d curves as the region before the first peak; the disordered flow region which is between the first peak in the dV_x/dF_d curve and the plateau in P_6; the moving stripe phase which is identified from the real space images and from $P_6 \geq 0.57$; and the moving labyrinth phase, identified from the real space images and from $P_6 \approx 0.5$. Figure 3 shows that the oriented stripe phase appears only above a critical disorder strength. In Fig. 4(a), we show P_6 at a fixed high drive of $F_d = 5.0$ for a series of simulations at the various f_p used in creating Fig. 3. Figure 4(a) clearly shows a jump near $f_p = 2.5$ indicating the transition from the moving labyrinth to the moving stripe state, as a function of f_p.

We have also performed simulations at fixed f_p and varied N_p, and find the same general phases. The moving stripe phase can be still realized with as few as $N_p = 50$

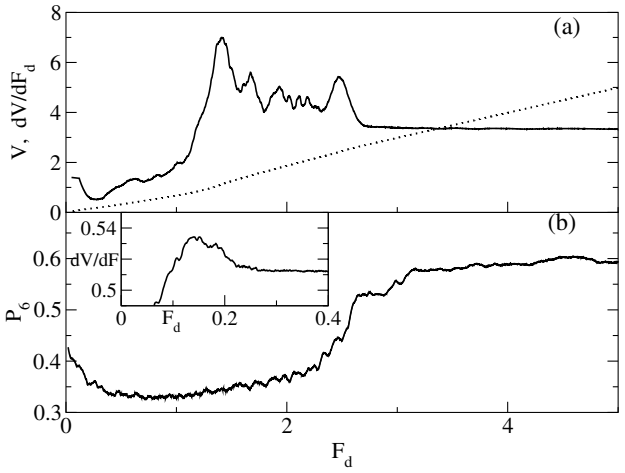

FIG. 2. (a) The velocity V_x vs F_d curve (dotted line), and dV_x/dF_d curve (solid line) for $f_p = 6.5$, $N_p = 400$, and $N_i = 1280$. (b) The corresponding sixfold coordination fraction P_6 vs F_d. Inset: The dV_x/dF_d curve for the same system as in (a), for a lower pinning strength, $f_p = 0.5$.

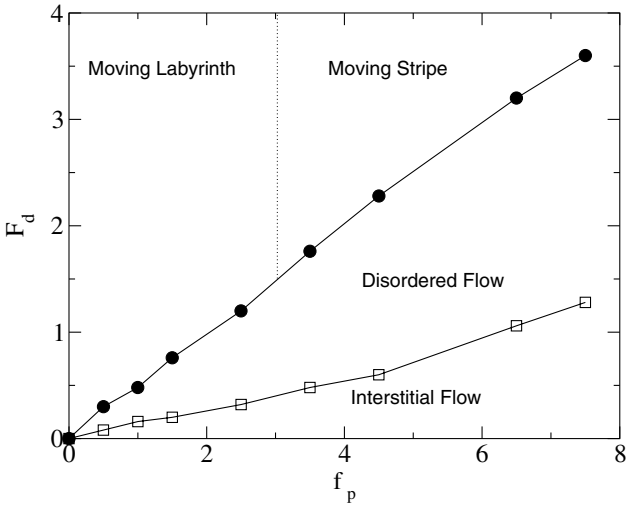

FIG. 3. The dynamic phase diagram for F_d vs f_p at fixed $N_i = 1280$ and $N_p = 400$. Four phases are delineated: the interstitial flow, disordered flow, moving labyrinth, and moving stripe phases.

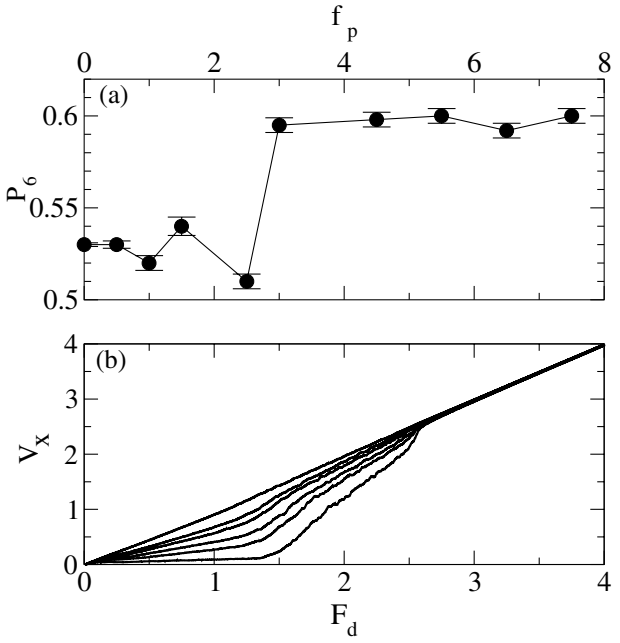

FIG. 4. (a) The sixfold coordination fraction P_6 vs f_p at a fixed value of $F_d = 5.0$, $N_i = 1280$, and $N_p = 400$ showing a crossover from the moving labyrinth phase to the moving stripe phase. (b) The velocity V_x vs F_d curve for fixed $f_p = 6.5$ and $N_i = 1280$ for varied N_p. From top to bottom, $N_p = 50$, 400, 600, 1400, and 2400.

pins. For $N_p < 50$, the flowing state consists of coexisting aligned stripes and labyrinths. In Fig. 4(b), we show the $V_x - F_d$ curves for varied N_p of 50 to 2400. The onset of the different phases as a function of drive changes little with increasing N_p. The value of V_x in the interstitial region continuously decreases since more particles can be pinned. At very high pin density, the interstitial region is lost and is replaced with a pinned region. The corresponding phase diagram would have the interstitial flow regime replaced by a pinned regime. For the high drives $F_d > 2.6$, all the curves become Ohmic in the free flow regime. We have also simulated systems with weaker pinning $f_p = 1.0$ and various N_p and find that the high drive state again becomes a moving labyrinth phase.

In summary, we have investigated the dynamic phases in a driven system with quenched disorder that forms a disordered stripe or labyrinth phase in equilibrium without pinning. For weak pinning, the system is disordered at low drives and reorders into a moving labyrinth phase at higher drives. Above a critical disorder strength, however, the system can reorder into a moving aligned stripe state. This stripe state is *more ordered than the unpinned equilibrium state*. Our results confirm that the dynamical reordering phenomenon studied in vortex lattices can be applied to other systems that do not form a triangular lattice in equilibrium. We have shown how the phases can be identified through transport properties and structure factors, and have mapped out the dynamical phase diagram as a function of disorder strength. Our results suggest that quenched disorder or other "obstacles" may be a useful way to engineer aligned domains in a labyrinth forming system. Additionally, our results will be useful for the interpretation of transport studies in, e.g., driven electron-liquid crystal systems.

This work was supported by DOE Contract No. W-7405-ENG-36.

[1] S. Bhattacharya and M. J. Higgins, Phys. Rev. Lett. **70**, 2617 (1993).
[2] A. E. Koshelev and V. M. Vinokur, Phys. Rev. Lett. **73**, 3580 (1994).
[3] P. Le Doussal and T. Giamarchi, Phys. Rev. B **57**, 11 356 (1998); T. Giamarchi and P. Le Doussal, Phys. Rev. Lett. **78**, 752 (1997).
[4] L. Balents, M. C. Marchetti, and L. Radzihovsky, Phys. Rev. Lett. **78**, 751 (1997); Phys. Rev. B **57**, 7705 (1998).
[5] S. Scheidl and V. M. Vinokur, Phys. Rev. E **57**, 2574 (1998).
[6] A. C. Marley, M. J. Higgins, and S. Bhattacharya, Phys. Rev. Lett. **74**, 3029 (1995); M. C. Hellerqvist *et al.*, *ibid.* **76**, 4022 (1996); Z. L. Xiao *et al.*, *ibid.* **85**, 3265 (2000).
[7] A. Duarte *et al.*, Phys. Rev. B **53**, 11 336 (1996); M. Marchevsky *et al.*, Phys. Rev. Lett. **78**, 531 (1997); F. Pardo *et al.*, Nature (London) **396**, 348 (1998).
[8] K. Moon, R. T. Scalettar, and G. T. Zimányi, Phys. Rev. Lett. **77**, 2778 (1996); S. Ryu *et al.*, *ibid.* **77**, 5114 (1996); M. C. Faleski *et al.*, Phys. Rev. B **54**, 12 427 (1996); S. Spencer and H. J. Jensen, *ibid.* **55**, 8473 (1997); C. J. Olson, C. Reichhardt, and F. Nori, Phys. Rev. Lett. **81**, 3757 (1998); A. B. Kolton, D. Dominguez, and N. Grønbech-Jensen, *ibid.* **83**, 3061 (1999).
[9] L. Balents and M. P. A. Fisher, Phys. Rev. Lett. **75**, 4270 (1995).
[10] C. Reichhardt *et al.*, Phys. Rev. Lett. **86**, 4354 (2001).
[11] T. Kawaguchi and H. Matsukawa, Phys. Rev. B **61**, R16 366 (2000); B. N. J. Persson, *Sliding Friction; Physical Principles and Application* (Springer, Heidelberg, 2000), 2nd ed.
[12] A. L. Barabasi and H. E. Stanley, *Fractal Concepts in Surface Growth* (Cambridge University Press, Cambridge, England, 1995).
[13] For a review, see M. Seul and D. Andelman, Science **267**, 476 (1995).
[14] M. Seul and R. Wolfe, Phys. Rev. A **46**, 7519 (1992).
[15] W. M. Gelbart and A. Ben Shaul, J. Phys. Chem. **100**, 13 169 (1996).
[16] J. Schmalian and P. G. Wolynes, Phys. Rev. Lett. **85**, 836 (2000).
[17] M. M. Fogler, A. A. Koulakov, and B. I. Shklovskii, Phys. Rev. B **54**, 1853 (1996); E. Fradkin and S. A. Kivelson, Phys. Rev. B **59**, 8065 (1999).
[18] B. P. Stojkovic *et al.*, Phys. Rev. Lett. **82**, 4679 (1999); Phys. Rev. B **62**, 4353 (2000).
[19] C. Reichhardt *et al.*, Europhys. Lett. (to be published).
[20] N. Grønbech-Jensen, Int. J. Mod. Phys. C **7**, 873 (1996); Comput. Phys. Commun. **119**, 115 (1999).
[21] M. Goulian and S. T. Milner, Phys. Rev. Lett. **74**, 1775 (1995).